NJC

Accepted Manuscript

This article can be cited before page numbers have been issued, to do this please use: T. K. Mondal, S. Gharami, K. Aich and L. Patra, *New J. Chem.*, 2018, DOI: 10.1039/C8NJ01212A.

ROYAL SOCIETY OF CHEMISTRY

rsc.li/njc

DOI: 10.1039/C8NJ01212A

Journal Name

ARTICLE

Detection and discrimination of Zn^{2+} and Hg^{2+} using a single molecular fluorescent probe

Received 00th January 20xx,
Accepted 00th January 20xx

DOI: 10.1039/x0xx00000x

www.rsc.org/

Saswati Gharami, Krishnendu Aich, Lakshman Patra and Tapan K. Mondal*

A new fluorescent probe (SAPH) has been introduced which shows specific sensing towards Zn^{2+} and Hg^{2+} in two different wavelength maxima at physiological pH. The probe shows a brilliant ratiometric red shift in emission spectra upon addition of Zn^{2+} at 678 nm while Hg^{2+} shows a turn-on ratiometric emission enhancement with a red shift at 647 nm. Job's plot confirms the 1:1 complexation for both Zn^{2+} and Hg^{2+}. Binding constants have been calculated using Benesi-Hildebrand equation and found to be 3.03×10^5 M^{-1} and 6.05×10^4 M^{-1} respectively for SAPH-Zn^{2+} and SAPH-Hg^{2+}. DFT and TDDFT studies are conducted with the probe to establish a similarity between theoretical and experimental outcomes.

Introduction

In recent days, the area of highly luminescent chemosensors has been of great interest owing to their various applications in photoelectronic diodes, biotechnology and memory system.[1-5] A large amount of fluorescent chemosensors which have been reported till are based on organic moieties as they are simple-to-use, cost effective and easy to handle.[6-9] The development of bifunctional fluorescent probes which selectively discriminates more than two metal ions or anions have been a very interesting area in the fluorescence studies recently.[10-16] Environmental contamination by heavy toxic metals is becoming a great threat in recent days due to the accumulation of these pollutants in water and foods which have led to various dangerous diseases in living beings.[17] Among the heavy metals, mercury is a highly toxic metal whose presence in environment causes great threat not only for the ecological system but also for the human health.[18] Mercury can be widely spread into the environment via various sources such as gold production, coal plants, thermometers, barometers, mercury lamps etc.[19] Even exposure to very small concentration of mercury can cause strong damage to the central nervous system.[20] Thus the long term accumulation of mercury in the human body can lead to various cognitive and motor disorders along with pulmonary edema, cyanosis, nephritic syndrome and Minamata disease.[21] So although many fluorescent probes are reported for the detection of Hg^{2+} in literature,[22] there is still an urgent need of developing a sensitive and appropriate Hg detection method. Zinc being the second most abundant transition metal after iron has various important roles in catalytic activity, neurological activity, gene transcription and cellular transport.[23] But unregulated zinc level in human body may lead to several dangerous diseases such as β-thalassemia, Friedreich's ataxia, and neurodegenerative diseases including Alzheimer's disease, Parkinson's disease and epilepsy.[24-26] The disorder of zinc level also leads to the probability of prostate cancer.[27] Furthermore detection of zinc is also very much needed for the sake of environment as it is a harmful metal pollutant too.[28] Therefore it is highly desirable and demandable to develop a powerful and sensitive analytical tool for the detection of Hg^{2+} and Zn^{2+} in environmental sample. There are many successful fluorescent probes reported to date which can selectively detects these two metal ions individually.[29,30] However, to detect one of these metals individually, there is some interference observed from the other one.[31] Therefore, it remains a challengeable task to design a single molecular probe that not only can recognize but also can discriminate these two metal ions belonging to the same group.

In this paper, we have investigated a simple idea for Zn^{2+} and Hg^{2+} specific probe design. So we have introduced a new fluorescent switch which exhibits fluorescence "turn-on" response towards Zn^{2+} and Hg^{2+} specifically in two different wavelength regions thereby discriminating the duo via one probe.

Experimental

General Procedures

All reagents and solvents used in this synthesis were purchased from Aldrich. All other organic chemicals and inorganic salts were available from commercial sources and used without further purification. ^1H and ^{13}C NMR spectra were recorded on Brucker 300 MHz instrument. For NMR spectra, $CDCl_3$ and DMSO-d_6 were used as solvents (mentioned

Department of Chemistry, Jadavpur University, Kolkata- 700032, India. E-mail: tapank.mondal@jadavpuruniversity.in

†Electronic Supplementary Information (ESI) available: [NMR and MS of all new compounds, Limit of detection determination, Quantum yield calculation etc.]. See DOI: 10.1039/x0xx00000x

View Article Online
DOI: 10.1039/C8NJ01212A

in the spectra for each case) using TMS as an internal standard. Chemical shifts are expressed in δ units and ^{1}H-^{1}H and ^{1}H-C coupling constants in Hz. HRMS mass spectra were recorded on Waters (Xevo G2 Q-TOF) mass spectrometer. Thin layer chromatography (TLC) was carried out using Merck 60 F_{254} plates with a thickness of 0.25 mm. Electronic spectra were taken on a PerkinElmer Lambda 750 spectrophotometer. Luminescence property was measured using Shimadzu RF-6000 fluorescence spectrophotometer at room temperature (298 K). Fluorescence lifetimes were measured using a time-resolved spectrofluorometer from IBH, UK.

Determination of fluorescence Quantum Yields (φ) of SAPH SAPH-Zn^{2+} and SAPH-Hg^{2+}

For measurement of the quantum yields of SAPH and its complexes with Zn^{2+} and Hg^{2+}, we recorded the absorbance of the compounds in acetonitrile solution. The emission spectra were recorded using the maximal excitation wavelengths, and the integrated areas of the fluorescence-corrected spectra were measured. The quantum yields were then calculated by comparison with fluorescein (φ_s = 0.79 in ethanol) as reference using the following equation:

$$\Phi_x = \Phi_s \times \left(\frac{I_x}{I_s}\right) \times \left(\frac{A_s}{A_x}\right) \times \left(\frac{n_x}{n_s}\right)^2$$

Where, x & s indicate the unknown and standard solution respectively, φ is the quantum yield, *I* is the integrated area under the fluorescence spectra, *A* is the absorbance and *n* is the refractive index of the solvent.

We calculated the quantum yields of SAPH and SAPH-Hg^{2+} and SAPH-Zn^{2+} using the above equation and the values are 0.01, 0.48 and 0.35 respectively.

Synthesis of 2-(hydrazono(phenyl)methyl)pyridine (1)

$N_2H_4.H_2O$ (excess) was added to the solution of 2-benzoyl pyridine (0.5 g, 2.73 mmol) in ethanol (10 mL). The mixture was stirred for 2 hour in refluxing condition. After cooling at room temperature, the solvent was evaporated under reduced pressure and water (10 mL) was added to the crude product and then extracted using dichloromethane (3 × 20 mL). Then the DCM portion was dried over the anhydrous sodium sulphate and evaporated. The evaporation of the solvent under reduced pressure affords a yellowish compound (0.43 g, 80%). The compound is pure enough and used directly for the next step without further purification.

^{1}H NMR (300 MHz, $CDCl_3$): δ 5.71 (s, 2H), 7.16 (t, J = 5.9 Hz, 1H), 7.36 (m, 4H), 7.47 (d, J= 7.1 Hz, 1H), 7.55 (t, J = 7.2 Hz, 1H), 7.64 (m, 1H), 8.55 (s, 1H).

HRMS: calculated for $C_{12}H_{12}N_3$ $[M + H]^+$ (m/z): 198.1031; found: 198.0953.

Synthesis of 5-(diethylamino)-2-((Z)-((E)-(phenyl(pyridin-2-yl)methylene)hydrazono)methyl) phenol(SAPH)

To a solution of compound 1 (0.5 g, 2.5 mmol) in ethanol (15 mL), 4-(diethylamino)-2-hydroxybenzaldehyde (0.49 g, 2.5 mmol) was added. The solution was refluxed for 4 h. The reaction mixture was cooled to room temperature and evaporated. After cooling to room temperature, the reaction mixture was kept to evaporate completely that yields a solid product which was purified through column chromatography using dichloromethane as eluent to afford SAPH (0.71 g, 75%) as orange yellow semi-solid.

^{1}H NMR (300 MHz, $CDCl_3$): δ 1.16 (t, J = 6.9 Hz, 6H), 3.34 (m, 4H), 6.08 (d, J = 9.0 Hz,1H), 6.21 (d, J = 9.0 Hz, 1H), 7.11 (d, J = 8.8 Hz, 1H), 7.30 (m, 1H), 7.38 (t, J = 6.4 Hz, 3H), 7.47 (m, 2H), 7.74 (m, 1H), 7.90 (m, 1H), 8.70 (t, J = 5.4 Hz, 1H), 11.59 (s, 1H).

^{13}C NMR (75 MHz, $CDCl_3$): δ 12.6, 44.6, 97.73, 104.0, 107.1, 123.8, 124.0, 124.6, 128.4, 128.9, 130.3, 133.9, 135.5, 136.5, 149.9, 151.9, 155.8, 162.0, 163.6, 164.0, 164.8.

HRMS: calculated for $C_{23}H_{25}N_4O$ $[M + H]^+$ (m/z) = 373.2028; found = 373.2209.

Synthesis of SAPH-Zn^{2+} complex

The receptor, SAPH (62 mg) and $ZnCl_2$ (23 mg) were mixed together and dissolved in 10 mL of acetonitrile. After refluxing for 1 hour the reaction mixture was cooled to room temperature. A wine red colored precipitate appeared which was filtered and dried. Single red colored crystals of the complex was obtained by slow diffusion of n-hexane into DCM solution.

^{1}H NMR (300 MHz, DMSO-d_6): δ 1.06 (t, J = 6.8 Hz, 6H), 6.28 (d, J = 8.9 Hz, 1H), 7.26 (d, J = 8.8 Hz, 3H), 7.44 (d, J = 6.5 Hz, 4H), 7.93 (m, 1H), 8.15 (s, 1H), 8.56 (s, 1H), 8.76 (s, 1H), 11.28 (s, 1H). **HRMS:** calculated for $C_{23}H_{23}N_4OClZn$ $[M + H]^+$ (m/z): 471.0919; found: 471.1536.

Synthesis of SAPH-Hg^{2+} complex

The receptor, SAPH (64 mg) and $HgCl_2$ (47 mg) were mixed together and dissolved in 8 mL of acetonitrile. After refluxing for 0.5 hour the reaction mixture was cooled to room temperature. An orange red coloured precipitate appeared which was filtered and dried. Single orange-red colored crystals of the complex was obtained by slow diffusion of n-hexane into DCM solution.

^{1}H NMR (300 MHz, DMSO-d_6): δ 1.06 (t, J = 6.8 Hz, 6H), 6.29 (d, J = 8.8 Hz, 1H), 7.27 (m, 3H), 7.46 (m, 4H), 7.95 (t, J = 7.8 Hz, 1H), 8.10 (d, J = 7.8 Hz, 1H), 8.59 (s, 1H), 8.78 (s, 1H), 11.24 (s, 1H). **HRMS:** calculated for $C_{23}H_{23}N_4OClHg$ $[M + H]^+$ (m/z): 609.1334 ; found: 609.1273.

Theoretical study

All calculations were performed with Gaussian 09 program package[32] with the support of the Gauss View visualization program. Full geometry optimizations were carried out using the density functional theory (DFT) method at the B3LYP[33] level for the compounds. All elements except zinc and mercury were assigned 6-31+G(d) basis set. The LanL2DZ basis set with effective core potential (ECP) set of Hay and Wadt[34] was used for both Zn and Hg. Vertical electronic excitations based on B3LYP optimized geometries were computed using the time-dependent density functional theory (TDDFT) formalism[35] in

DOI: 10.1039/C8NJ01212A

acetonitrile using conductor-like polarizable continuum model (CPCM).[36]

Results and discussion

The chemical structures of SAPH and its Zn^{2+} and Hg^{2+} complexes are confirmed by ^{1}H and ^{13}C NMR spectroscopy and ESI mass spectrometry. Compound 1 was obtained via addition of excess $N_2H_4.H_2O$ to the ethanolic solution of 2-benzoyl pyridine with the yield of 80%. Synthesis of the probe, SAPH involved reflux condensation of compound 1 and 4-(diethylamino)-2-hydroxybenzaldehyde (2) in ethanol (scheme 1). The yield is 75%.

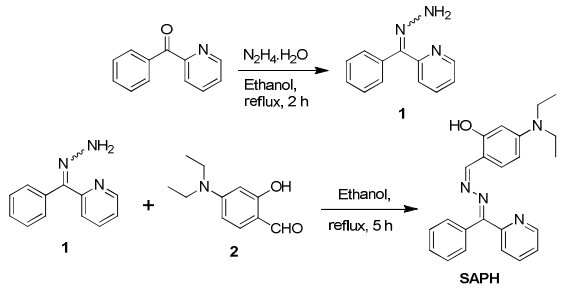

Scheme 1. Synthetic scheme for the probe, SAPH

Photophysical Properties

The absorbance and fluorescence properties of SAPH were studied in acetonitrile-water (1/1, v/v) solution at 25°C under physiological pH (10 mM HEPES buffer, pH=7.4). The absorption spectral changes of SAPH upon gradual addition of different metal ions were recorded. The UV-vis spectrum of SAPH itself (10 μM) in CH_3CN/H_2O (1/1, v/v) shows a peak at 408 nm. Upon gradual addition of Hg^{2+} to the solution of the probe, the band at 408 nm decreases along with formation of a new peak at around 467 nm and three distinct isosbestic points at 287 nm, 341 nm and 440 nm respectively (Fig. 1a). Consequently, the light yellow solution of the probe turns to orange (Fig. 1a, Inset). In case of Zn^{2+}, the band at 408 nm decreases on gradual addition of Zn^{2+} while a new band is generated at 479 nm. Here three well defined isosbestic points at 283 nm, 351 nm and 439 nm were observed (Fig. 1b) accompanying a color change from light yellow to red which was easily detectable via naked eye. The change in absorption spectra of SAPH in presence of Hg^{2+} and Zn^{2+} may be due to the internal charge transfer (ICT) process. Color change of SAPH from light yellow to orange and red (i.e bathochromic spectral shift) in presence of Hg^{2+} and Zn^{2+} respectively also suggests that the ICT process occurs after complexation. To establish the selectivity of the probe to these two metal cations, the absorption spectral changes of the probe in presence of other metal cations were recorded too which shows that only Cu^{2+} and Ni^{2+} undergo changes in absorption spectra (ESI, Fig. S10).

SAPH, upon excitation at 415 nm, gives a weak emission band (ϕ = 0.01) at 500 nm in CH_3CN /H_2O (1/1, v/v) solution. With increasing concentration of Hg^{2+}, the peak of SAPH at 500 nm gradually vanishes out and a new red shifted band is generated at 647 nm and increases regularly (Fig. 2a). Almost 80 fold of enhancement in emission intensity is observed after addition of Hg^{2+} to SAPH solution. Consequently, enhancement of fluorescence quantum yield from 0.01 to 0.48 is observed. Similarly, the gradual addition of Zn^{2+} to the CH_3CN /H_2O (1/1, v/v) solution of the probe results in an increase of emission intensity of the relatively weak emission band at 500 nm with a ratiometric red shift at 678 nm (Fig. 2b). After addition of Zn^{2+}, the emission intensity of SAPH increases to about 61 fold thereby accounting for a quantum yield (ϕ = 0.35) higher than that of SAPH (ϕ = 0.01). These emission changes may also be attributed to ICT process. The increase in the emission intensity may be due to the chelation induced enhanced emission (CHEF) process.

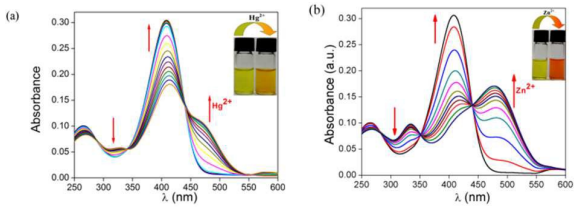

Fig. 1. Change in UV-Vis spectrum of SAPH (10 μM) upon addition of (a) Hg^{2+} (0-20 μM) and (b) Zn^{2+} (0-20 μM) in CH_3CN/H_2O (1/1, v/v) (10 mM HEPES buffer, pH=7.4). (Inset shows the change in colour in visible light)

To evaluate its specific selectivity profile towards Zn^{2+} and Hg^{2+}, a group of metal ions such as Na^{+}, K^{+}, Co^{2+}, Ni^{2+}, Cu^{2+}, Cd^{2+}, Mn^{2+}, Al^{3+}, Fe^{2+}, Ag^{+}, Ca^{2+}, Cr^{3+}, Fe^{3+}, Mg^{2+} and Pb^{2+} were chosen as the competing ions to perform the fluorescence tests and it is found that none other metal ions caused any significant change in emission profile (Fig. 3). Therefore SAPH can serve as a selective fluorescent probe for both Zn^{2+} and Hg^{2+} ions in the presence of other competing metal ions at physiological pH. An interference experiment was carried out by measuring the emission intensity of SAPH (10 μM) in presence of other metal ions (20 μM) in order to study the selectivity of the probe. It is observed that the fluorescence enhancement of SAPH is specific towards both Hg^{2+} (Fig. 4a) and Zn^{2+} (Fig. 4b) respectively and is hardly affected by the presence of other metal cations.

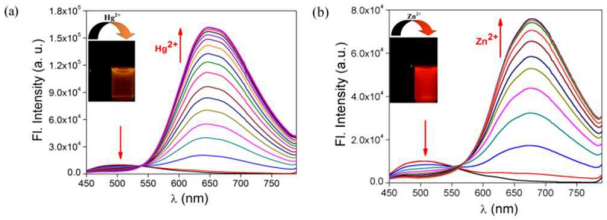

Fig. 2. Change in emission spectra of SAPH (10 μM) upon gradual addition of (a) Hg^{2+} (0-20 μM) and (b) Zn^{2+} (0-20 μM) in CH_3CN /H_2O (1/1, v/v) (10 mM HEPES buffer, pH=7.4). (Inset shows the change in colour in UV-chamber)

View Article Online
DOI: 10.1039/C8NJ01212A

Now in order to quantify the stoichiometry of the complex of SAPH with these metal ions duo, Job's plot analysis was carried out. The maxima appears at a mole fraction of 0.5 for each of the metal ions, which correspond to the 1:1 complex formation of SAPH and Hg^{2+} and Zn^{2+} respectively (ESI, Fig. S11a and S11b). The HRMS of SAPH shows a peak at m/z 373.2209 possibly for $[SAPH + H]^+$ (ESI,† Fig. S5) whereas the Zn^{2+} complex and Hg^{2+} complex show peaks at m/z 471.1536 and 609.1273 respectively accounting for the probable composition $[SAPH + Zn^{2+} + H]^+$ and $[SAPH + Hg^{2+} + H]^+$, which also prove the mononuclear complex of SAPH with Zn^{2+} and Hg^{2+} (Fig. 5 and ESI,† Fig. S7 and S9). The association constant (K_a) of SAPH for Hg^{2+} was determined to be 6.05×10^4 M^{-1} from Benesi-Hildebrand plot using the data obtained from fluorescence titration (ESI, Fig. S12a). Similarly for Zn^{2+}, the K_a was also calculated and was found to be 3.03×10^5 M^{-1} (ESI, Fig. S12b) respectively.

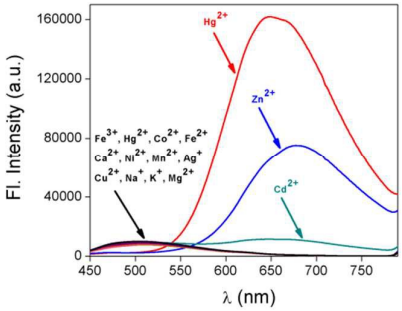

Fig. 3. Change in emission intensity of SAPH (10 μM) upon addition of different metal ions (20 μM) in CH_3CN/H_2O (1/1, v/v) (HEPES buffer, pH=7.4).

The emission intensity of the probe (SAPH) at 647 nm increased linearly with the amount of Hg^{2+} added in the range of 0 to 11 μM (R^2 =0.9952) (ESI,† Fig. S13a). The limit of detection of SAPH for Hg^{2+} was determined from the emission spectral change upon addition of Hg^{2+} to be 4.98×10^{-10} M (ESI,† Fig. S14a). Similarly for Zn^{2+}, the emission intensity of SAPH increased linearly at 678 nm in the range of 0 to 6 μM (R^2 =0.9870) (ESI, Fig. S13b) and detection limit was calculated to be 1.23×10^{-9} M (ESI,† Fig. S14b).

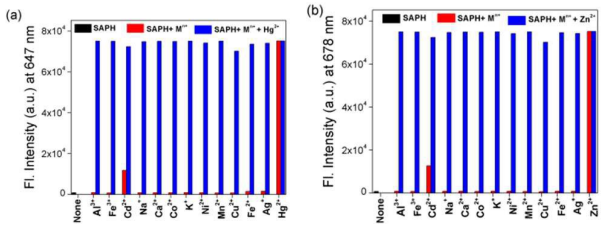

Fig. 4. Bar diagram representation of the relative emission intensity of SAPH upon addition of various metals (10 μM) in CH_3CN:H_2O (1:1, v/v) (HEPES buffer, pH=7.4) (red bars) and (a) Hg^{2+} (20 μM) in presence of other metal ions (navy blue bars) and (b) Zn^{2+} (20 μM) in presence of other metal ions (navy blue bars)

pH study

The acid-base titration of SAPH was carried out in absence and presence of both Hg^{2+} and Zn^{2+}. The study clearly reveals that SAPH does not undergo any significant change in emission intensity at 500 nm within the pH range of 2-12 thereby suggesting that the probe is sufficiently stable in this pH range. On addition of Hg^{2+} in the solution of SAPH, the emission intensity increases rapidly within the pH range of 6-10 thus establishing the fact that SAPH can efficiently detect Hg^{2+} within the aforementioned pH range (ESI, Fig. S15a). The increase in emission intensity may be due to the sufficiently strong complexation between SAPH and Hg^{2+} within the pH range of 6-10. On further increase in pH, the complexation process is inhibited thereby observing decrease in the emission intensity. Similarly, on addition of Zn^{2+} into the SAPH solution, the emission intensity again increases with increasing pH and acquires maxima at pH 7 but further increase in pH results in sharp drop of emission intensity within the pH range of 8-10 thus suggesting the dissociation of the SAPH-Zn^{2+} complex (ESI, Fig. S15b). Hence the probe SAPH can detect Zn^{2+} in the neutral pH range with brilliant efficiency.

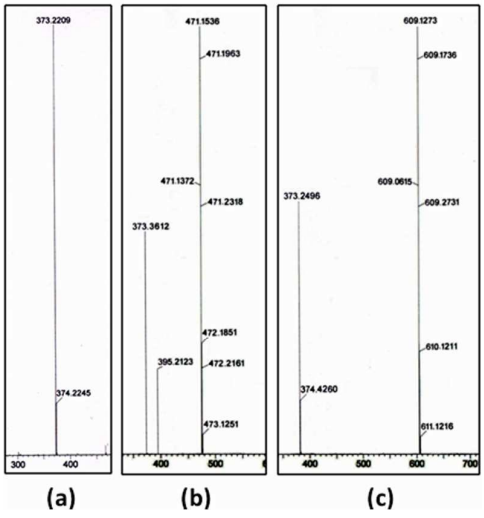

Fig. 5. Partial HRMS spectra of (a) SAPH, (b) SAPH-Zn^{2+} and (c) SAPH-Hg^{2+}

Computational study

To further understand the relationship between the structural changes of SAPH and its complexes with Zn^{2+} and Hg^{2+}, we carried out the density functional theory (DFT) calculations with the B3LYP/6-31+G(d) method using the Gaussian 09 program. Optimized structures of the probe SAPH, SAPH-Zn^{2+} and SAPH-Hg^{2+} complexes are shown in Fig. 6. Selected highest occupied molecular orbitals (HOMOs) and lowest unoccupied molecular orbitals (LUMOs) of SAPH and its Zn^{2+} and Hg^{2+} complexes are presented in Figs. S16-18. Energy and % of composition of selected molecular orbitals of SAPH-Zn^{2+} and SAPH-Hg^{2+} are summarized in Table S1 and Table S2 respectively. The HOMO-LUMO energy gap of SAPH (3.35 eV) is significantly reduced in SAPH-Zn^{2+} (2.82 eV) and SAPH-Hg^{2+} (2.98 eV) complexes which reflects in the shifting of low energy band in the complexes. Further, to interpret the electronic transitions, time dependent density functional theory (TDDFT) was carried out to the optimized geometries of

View Article Online
DOI: 10.1039/C8NJ01212A

the compounds. The low energy transition for SAPH at 425 nm ($\lambda_{expt.}$, 408 nm) corresponds to HOMO → LUMO transition. For, SAPH-Zn^{2+} and SAPH-Hg^{2+} the low energy band shifted to 489 nm ($\lambda_{expt.}$, 479 nm) and 482 nm ($\lambda_{expt.}$, 467 nm) respectively (Table S3).

Fig. 6. Optimized structures of (a) SAPH, (b) SAPH-Zn^{2+} and (c) SAPH-Hg^{2+} by DFT/B3LYP/6-31G(d) method

Test-kit for the detection of Hg^{2+} and Zn^{2+}

Stimulated by the distinct discrimination of SAPH towards Hg^{2+} and Zn^{2+}, we decided to bring out some potential application by using the single molecule as a handy portable tool for sensing of these two metal cations. This experiment has huge importance as without the aid of any instruments, it can give some vital qualitative data. So in order to fulfil this experiment, few thin-layer chromatography (TLC) plates were prepared and then immersed into the solution of SAPH (2×10^{-4} M) in acetonitrile and then kept for few minutes to evaporate the solvent, followed by dipping the TLC plates to Zn^{2+} (2×10^{-3} M) and Hg^{2+} (2×10^{-3} M) solutions and then again evaporate the solvent. The colour of the TLC plates show the change from light yellow to orange-yellow under ambient light for both the metal ions whereas colorless to brown in case of Zn^{2+} under UV light and colorless to bright red for Hg^{2+} (Fig. 7).

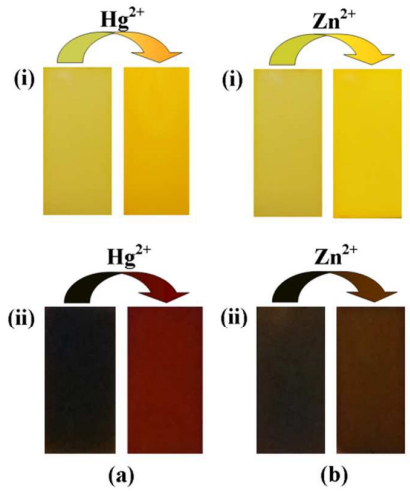

Fig. 7: Photographs of TLC plates after immersion in the SAPH-acetonitrile solution and after immersion in (a) SAPH-Hg^{2+} and (b) SAPH-Zn^{2+} acetonitrile solution (i) taken in ambient light and (ii) under hand-held UV light. Excitation wavelength of the UV light is 360 nm. [SAPH] = 2×10^{-4} M, [Hg^{2+}] and [Zn^{2+}] = 2×10^{-3} M.

Conclusions

So we reported here the synthesis of a new fluorescent ratiometric probe which showed selective fluorescence response upon complexation with two same group metals viz. Zn^{2+} and Hg^{2+} ions. This newly developed probe SAPH exhibits a noteworthy ratiometric emission enhancement showing a red-shift in the emission maxima at 647 nm along with a visible colour change from light yellow to orange on addition of increased concentration of Hg^{2+} while in presence of Zn^{2+}, SAPH shows similar red shift at 678 nm along with a color change of light yellow to red in visible region. Moreover, the present fluorescent probe shows high selectivity towards Hg^{2+} and Zn^{2+} over other metal cations with sufficiently low detection limits of the order of 10^{-10} and 10^{-9} M respectively in physiological conditions.

Conflicts of interest

There are no conflicts to declare.

Acknowledgements

Authors thank the CSIR (No. 01(2831)/15/EMR-II) and SERB (No. YSS/2015/001533), New Delhi, India for financial supports. K.A thanks DST-SERB for providing the funding. S.G and L.P acknowledge UGC, New Delhi, India for providing them fellowships.

Notes and references

1 Q. Xu, H. M. Duong, F. Wudl and Y. Yang, *Appl. Phys. Lett.*, 2004, **85**, 3357.
2 J. Xiao, B. Yang, J. I. Wong, Y. Liu, F. Wei, K. J. Tan, X. Teng, Y. Wu, L. Huang, C. Kloc, F. Boey, J. Ma, H. Zhang, H. Y. Yang and Q. Zhang, *Org. Lett.*, 2011, **13**, 3004.
3 J. Xiao, Y. Divayana, Q. Zhang, H. M. Doung, H. Zhang, F. Boey, X. W. Sunb and F. Wudl, *J. Mater. Chem.*, 2010, **20**, 8167.
4 J. Xiao, S. Liu, Y. Liu, L. Ji, X. Liu, H. Zhang, X. Sun and Q. Zhang, *Chem. Asian J.*, 2012, **7**, 561.
5 Q. Zhang, Y. Divayana, J. Xiao, Z. Wang, E. R. T. Tiekink, H. M. Doung, H. Zhang, F. Boey, X. W. Sun and F. Wudl, *Chem. Eur. J.*, 2010, **16**, 7422.
6 C.-B. Huang, L. Xu, J.-L. Zhu, Y.-X. Wang, B. Sun, X. Li and H.-B. Yang, *J. Am. Chem. Soc.*, 2017, **139**, 9459.
7 Z. Xu, G. Li, Y.-Y. Ren, H. Huang, X. Wen, Q. Xu, X. Fan, Z. Huang, J. Huang and L. Xu, *Dalton Trans.*, 2016, **45**, 12087.
8 H.-I. Un, S. Wu, C.-B. Huang, Z. Xu and L. Xu, *Chem. Commun.*, 2015, **51**, 3143.
9 H.-I. Un, C.-B. Huang, J. Huang, C. Huang, T. Jia and L. Xu, *Chem. Asian J.*, 2014, **9**, 3397.
10 L. Xu, Y. Xu, W. Zhu, B. Zeng, C. Yang, B. Wu and X. Qian, *Org. Biomol. Chem.*, 2011, **9**, 8284.
11 L. Xu, Y. Xu, W. Zhu, X. Sun, Z. Xu and X. Qian, *RSC Adv.*, 2012, **2**, 6323.
12 L. Xu, Y. Xu, W. Zhu, Z. Xu, M. Chen and X. Qian, *New J. Chem.*, 2012, **36**, 1435.
13 C.-B. Huang, H.-R. Li, Y. Luoc and L. Xu, *Dalton Trans.*, 2014, **43**, 8102.
14 Y.-W. Wang, Y.-X. Hua, H.-H. Wu, X. Sun, Y. Peng, *Chin. Chem. Lett.*, 2017, **28**, 1994.
15 Y.-W. Wang, S.-B. Liu, W.-J. Ling and Y. Peng, *Chem. Commun.*, 2016, **52**, 827.

View Article Online
DOI: 10.1039/C8NJ01212A

16 16. X. Sun, Y.-W. Wang and Y. Peng, *Org. Lett.*, 2012, **14**, 3420.
17 P. Zhuang, M. McBride, H. Xia, N. Li and Z. Li, *Sci. Total Environ.*, 2009, **407**, 1551.
18 (*a*) T. C. Hutchinson, K. M. Meema and J. Wiley, New York, 1987; (*b*) G. H. Scoullos, M. J. Vonkeman, L. Thorton and Z. Makuch, In *Mercury, Cadmium, and Lead: Handbook for Sustainable Heavy Metals Policy and Regulation (Environment & Policy*, V. 31), Kluwer Academic, Norwell, MA, 2001; (*c*) C. J. Coester, *Anal. Chem.*, 2005, **77**, 3737; (*d*) S. D. Richardson and T. A. Temes, *Anal. Chem.*, 2005, **77**, 3807.
19 F. Di Natale, A. Lancia, A. Molino, M. Di Natale, D. Karatza and D. Musmarra, *J. Hazard. Mater.*, 2006, **132**, 220.
20 C. M. L. Carvalho, E. -H. Chew, S. I. Hashemy, J. Lu and A. Holmgren, *J. Biol. Chem.*, 2008, **283**, 11913.
21 (a) T. W. Clarkson, L. Magos and G. J. Myers, *N. Engl. J. Med.*, 2003, **349**, 1731; (b) S. Ekino, M. Susa, T. Ninomiya, K. Imamura and T. Kitamura, *J. Neurol. Sci.*, 2007, **262**, 131; (c) D. A. Geier and M. R. Geier, *J. Toxicol. Environ. Health, Part A*, 2007, **70**, 837; (d) M. Korbas, S. R. Blechinger, P. H. Krone, I. J. Pickering and G. N. George, *Proc. Natl. Acad. Sci. U. S. A.*, 2008, **105**, 12108.
22 (a) H.-I. Un, C.-B. Huang, C. Huang, T. Jia, X.-L. Zhao, C.-H. Wang, L. Xu and H.-B. Yang, *Org. Chem. Front.*, 2014, **1**, 1083; (b) Y.-K. Yang, K.-J. Yook and J. Tae, *J. Am. Chem. Soc.*, 2005, **127**, 16760; (c) A. Caballero, R. Martínez, V. Lloveras, I. Ratera, J. Vidal-Gancedo, K. Wurst, A. Tárrage, P. Molina and J. Veciana, *J. Am. Chem. Soc.*, 2005, **127**, 15666; (d) M. H. Lee, J.-S. Wu, J. W. Lee, J. H. Jung and J. S. Kim, *Org. Lett.*, 2007, **9**, 2501; (e) X. Zhang, Y. Xiao and X. Qian, *Angew. Chem. Int. Ed.*, 2008, **47**, 8025; (f) M. Santra, D. Ryu, A. Chatterjee, S.-K. Ko, I. Shin and K. H. Ahn, *Chem. Commun.*, 2009, **16**, 2115; (g) A. Mitra, A. K. Mittal and C. P. Rao, *Chem. Commun.*, 2011, **47**, 2565; (s) H. Zheng, X.-J. Zhang, X. Cai, Q.-N. Bian, M. Yan, G.-H. Wu, X.-W. Lai and Y.-B. Jiang, *Org. Lett.*, 2012, **14**, 1986; (h) W. Xuan, C. Chen, Y. Cao, W. He, W. Jiang and W. Wang, *Chem. Commun.*, 2012, **48**, 7292; (i) K. Bera, A. K. Das, M. Nag and S. Basak, *Anal. Chem.*, 2014, **86**, 2740; (j) S. Ozturk and S. Atilgan, *Tetrahedron Lett.*, 2014, **55**, 70; (k) E. M. Nolan and S. J. Lippard, *J. Am. Chem. Soc.*, 2003, **125**, 14270.
23 (a) C. J. Frederickson, J. -Y. Koh, A. I. Bush, *Nat. Rev. Neurosci.*, 2005, **6**, 449; (b) P. J. Fraker and L. E. King, *Annu. Rev. Nutr.*, 2004, **24**, 277.
24 J. Lai, A. Moxey, G. Nowak, K. Vashum, K. Bailey and M. McEvoy, *J. Affect. Disord.*, 2012, **136**, 31.
25 J. H. Weiss, S. L. Sensi and J. Y. Koh, *Phamacol. Sci.*, 2000, **21**, 395.
26 M. Maes, N. D. Vos, P. Demedts, A. Wauters and H. Neels, *J. Affect. Disord.*, 1999, **56**, 189.
27 (a) N. Dubi, L. Gheber, D. Fishman, I. Sekler and M. Hershfinkle, *Carcinogenesis*, 2008, **29**, 1692; (b) M. Sztalmachova, M. Hlavna, J. Gumulec, M. Holubova, P. Babula, J. Balvan, J. Sochor, V. Tanhauserova, M. Raudenska, S. Krizkova, V. Adam, T. Eckschlager, R. Kizek and M. Masarik, *Oncol. Rep.*, 2012, **28**, 806.
28 A. Voegelin, S. Poster, A. C. Scheinost, M. A. Marcus and R. Kretzsch-mar, *Environ. Sci. Technol.*, 2005, **39**, 6616.
29 For Hg^{2+} see: (a) P. Srivastava, S. S. Razi, R. Ali, R. C. Gupta, S. S. Yadav, G. Narayan and A. Misra, *Anal. Chem.*, 2014, **86**, 8693. (b) X. Zhang, H. Zhao, X. Cao, N. Feng, D. Tian and H. Li, *Org. Biomol. Chem.*, 2013, **11**, 8262. (c) B.-X. Shen and Y. Qian, *Sens. Actuators, B* 2017, **239**, 226. (d) U. Ghosh, S. S. Bag and C. Mukherjee, *Sens. Actuators, B* 2017, **238**, 903. (e) Z. Ruan, Y. Shan, Y. Gong, C. Wang, F. Ye, Y. Qiu, Z. Liang and Z. Li, *J. Mater. Chem. C*, 2018, **6**, 773. (f) A. Petdum, W. Panchan, J. Sirirak, V. Promarak, T. Sooksimuang and N. Wanichacheva, *New J. Chem.*, 2018, **42**, 1396. (g) M. Ozdemir, *Sens. Actuators, B* 2017, **249**, 217. (h) D. Mahajan, N. Khairnar, B. Bondhopadhyay, S. K. Sahoo, A. Basu, J. Singh, N. Singh, R. Bendre and A. Kuwar, *New J. Chem.*, 2015, **39**, 3071.
30 For Zn^{2+} see: (a) D. Sarkar, A. K. Pramanik and T. K. Mondal, *RSC Adv.*, 2014, **4**, 25341; (b) D. Sarkar, A. K. Pramanik and T. K. Mondal, *RSC Adv.*, 2015, **5**, 7647; (c) Y. Xu, L. Xiao, S. Sun, Z. Pei, Y. Pei and Y. Pang, *Chem. Commun.*, 2014, **50**, 7514; (d) N. Khairnar, K. Tayade, S. K. Sahoo, B. Bondhopadhyay, A. Basu, J. Singh, N. Singh, V. Gite and A. Kuwar, *Dalton Trans.*, 2015, **44**, 2097; (e) K. Aich, S. Goswami, S. Das and C. Das Mukhopadhyay, *RSC Adv.*, 2015, **5**, 31189; (f) B. K. Datta, D. Thiyagarajan, S. Samanta, A. Ramesh and G. Das, *Org. Biomol. Chem.*, 2014, **12**, 4975; (g) J. Pancholi, D. J. Hodson, K. Jobe, G. A. Rutter, S. M. Goldup and M. Watkinson, *Chem. Sci.*, 2014, **5**, 3528; (h) N. Lin, Q. Zhang, X. Xia, M. Liang, S. Zhang, L. Zheng, Q. Cao and Z. Ding, *RSC Adv.*, 2017, **7**, 21446. (i) W.-K. Dong, S. F. Akogun, Y. Zhang, Y.-X. Sun, X.-Y. Dong, *Sens. Actuators, B*, 2017, **238**, 723. (j) Z. Shi, Y. Tu and S. Pu, *RSC Adv.*, 2018, **8**, 6727.
31 (a) X. Wan, S. Yao, H. Liu and Y. Yao, *J. Mater. Chem. A*, 2013, **1**, 10505. (b) Z. Wu, Y. Zhang, J. S. Ma and G. *Inorg Chem.*, 2006, **45**, 3140. (c) J. M. Jung, J. J. Lee, E. Nam, M. H. Lim, C. Kim and R. G. Harrison, *Spectrochim. Acta, Part A*, 2017, **178**, 203.
32 Gaussian 09, Revision D.01, M. J. Frisch, G. W. Trucks, H. B. Schlegel, G. E. Scuseria, M. A. Robb, J. R. Cheeseman, G. Scalmani, V. Barone, B. Mennucci, G. A. Petersson, H. Nakatsuji, M. Caricato, X. Li, H. P. Hratchian, A. F. Izmaylov, J. Bloino, G. Zheng, J. L. Sonnenberg, M. Hada, M. Ehara, K. Toyota, R. Fukuda, J. Hasegawa, M. Ishida, T. Nakajima, Y. Honda, O. Kitao, H. Nakai, T. Vreven, J. A. Montgomery, Jr., J. E. Peralta, F. Ogliaro, M. Bearpark, J. J. Heyd, E. Brothers, K. N. Kudin, V. N. Staroverov, R. Kobayashi, J. Normand, K. Raghavachari, A. Rendell, J. C. Burant, S. S. Iyengar, J. Tomasi, M. Cossi, N. Rega, J. M. Millam, M. Klene, J. E. Knox, J. B. Cross, V. Bakken, C. Adamo, J. Jaramillo, R. Gomperts, R. E. Stratmann, O. Yazyev, A. J. Austin, R. Cammi, C. Pomelli, J. W. Ochterski, R. L. Martin, K. Morokuma, V. G. Zakrzewski, G. A. Voth, P. Salvador, J. J. Dannenberg, S. Dapprich, A. D. Daniels, Ö. Farkas, J. B. Foresman, J. V. Ortiz, J. Cioslowski and D. J. Fox, Gaussian, Inc., Wallingford CT, 2009.
33 (a) A. D. Becke, *J. Chem. Phys.*, 1993, **98**, 5648. (b) C. Lee, W. Yang and R. G. Parr, *Phys. Rev. B*, 1988, **37**, 785.
34 P. J. Hay and W. R. Wadt, *J. Chem. Phys.*, 1985, **82**, 299.
35 (a) R. Bauernschmitt and R. Ahlrichs, *Chem. Phys. Lett.* 1996, **256**, 454. (b) R.E. Stratmann, G.E. Scuseria and M.J. Frisch, *J. Chem. Phys.* 1998, **109**, 8218. (c) M.E. Casida, C. Jamorski, K.C. Casida and D.R. Salahub, *J. Chem. Phys.* 1998, **108**, 4439.
36 (a) V. Barone and M. Cossi, *J. Phys. Chem. A* 1998, **102**, 1995. (b) M. Cossi and V. Barone, *J. Chem. Phys.* 2001, **115,** 4708. (c) M. Cossi, N. Rega, G. Scalmani and V. Barone*, J. Comput. Chem*. 2003, **24**, 669.

View Article Online
DOI: 10.1039/C8NJ01212A

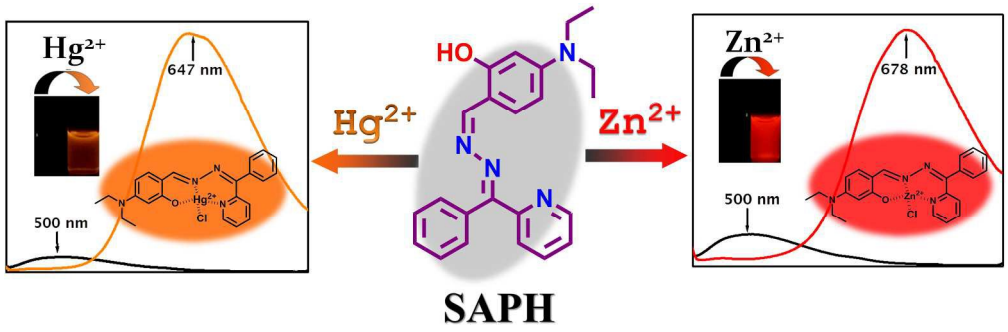

1002x321mm (77 x 77 DPI)